



Modeling age of information in a cooperative slotted Aloha network

Kaveh Vaezi¹ · Nail Akar¹ · Ezhan Karaşan¹

Accepted: 6 March 2023

© The Author(s), under exclusive licence to Springer Science+Business Media, LLC, part of Springer Nature 2023

Abstract

In this paper, we study a slotted Aloha cooperative network where a source node and a relay node send status updates of two underlying stochastic processes to a common destination. Additionally, the relay node cooperates with the source by accepting its packets for further re-transmissions using probabilistic acceptance and relaying. We obtain the exact steady state distributions of Age of Information (AoI) and Peak AoI sequences of both nodes using Quasi-Birth-Death Markov chains. The analytical model is first validated by simulations and then used to obtain optimal cooperation policies when transmission probabilities are fixed. Subsequently, we study the more general problem of joint optimization of the transmission probabilities and cooperation level between the source and relay, with detailed numerical examples.

Keywords Age of information · Peak age of information · Slotted Aloha · Cooperative networks · QBD Markov chains

1 Introduction

In wireless status update systems, individual nodes send wirelessly the status of certain underlying stochastic processes towards a common destination (or monitor) in the form of information packets. In such systems, the timeliness of the status updates at the destination is of crucial importance. For the purpose of quantifying the timeliness, for a given node, the Age of Information (AoI) sequence is defined as the elapsed time since the generation instance of the last packet that has been delivered to the destination [1]. As a result, this AoI sequence is a cyclic sequence which increases steadily in a cycle but is subject to abrupt downward jumps at the end of that cycle, due to reception of a new packet. The Peak AoI (PAoI) sequence is obtained by concatenating the per-cycle peak values of the AoI sequence [2]. The expected values of the stationary AoI and PAoI sequences in discrete-time and of the AoI and

PAoI processes in continuous-time have been extensively studied in the literature for a wide variety of communication scenarios. However, their higher order moments or distributions are sought to a lesser extent; see the recent surveys on AoI [3, 4] and the references therein. On the other hand, cooperative scenarios are of great interest in a wide range of wireless networks such as IoT systems, next generation communication networks, sensor networks and so on, due to their ability to improve the network performance in terms of throughput and delay. However, AoI-related metrics have not been extensively studied in cooperative status update systems where certain nodes transmit their time-sensitive packets cooperatively to a destination.

In this paper, we investigate AoI and PAoI in a cooperative slotted Aloha network in which a pair of source and relay nodes send status updates of the so-called source and relay processes, respectively, to a common destination in a timely manner; see Fig. 1. Moreover, the relay node attempts to reduce the AoI of the source node by devoting its own transmission resources for relaying the unsuccessfully transmitted packets of the source node, at the expense of increasing the AoI of the relay node itself. In the studied setting, the relay node controls the level of cooperation by adopting two probabilistic policies namely the admission and relaying policies, the combination of these two policies being referred to as the cooperation policy. This cooperative scheme being as simple as it

✉ Nail Akar
akar@ee.bilkent.edu.tr

Kaveh Vaezi
k.vaezi@gmail.com

Ezhan Karaşan
ezhan@ee.bilkent.edu.tr

¹ Department of Electrical and Electronics Engineering, Bilkent University, Ankara, Turkey

seems, can be considered as the core mechanism of more complex networks, and has been largely used in various existing studies [5–8]. The main contributions of this paper are as follows:

- To the best of our knowledge, the cooperative slotted Aloha cooperative network is studied in a general setting for the first time, from an age of information perspective. More specifically, in the studied scheme, transmissions of the source and relay nodes use random access. Also, the packets of the source may reach the destination via direct transmission or the two-hop relay link.
- The exact distributions of the AoI and PAoI sequences associated with the source and relay nodes are obtained in this general setting using Quasi-Birth-Death (QBD) Markov chains.

The rest of the paper is organized as follows. Section 2 presents the related work. Section 3 presents preliminaries for QBD Markov chains which will be instrumental for the remainder of the paper. Section 4 details the system model. The steady state distributions of the source and relay AoI and PAoI sequences are obtained in Sect. 5. In Sect. 6, numerical results are presented. Finally, Sect. 7 concludes the paper.

2 Related work

The introduction of the AoI concept in [1, 9] has recently caused a surge of interest in AoI-related research. In the earlier works, AoI is generally studied from a continuous-time queuing systems viewpoint. In [1], the average AoI was obtained for $M/M/1$, $M/D/1$ and $D/M/1$ queues with First-Come-First-Served (FCFS) discipline and optimal arrival rates are obtained for minimizing the average AoI. The reference [10] studied the AoI and PAoI in FCFS $M/M/1/1$ and $M/M/1/2$ queues as well as the non-preemptive Last-Come-First-Served (LCFS) $M/M/1/2^*$ queue whereas [11] derived a general formula for the stationary

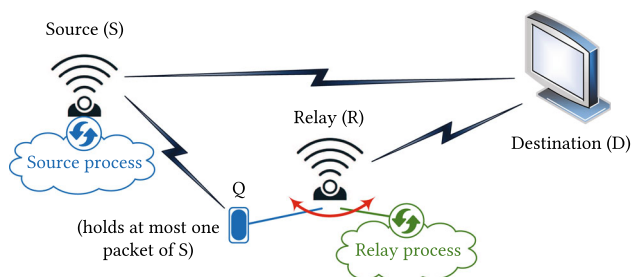


Fig. 1 The studied two-node cooperative slotted Aloha-based scenario

distribution of the AoI in a very general single-source setting. The exact distributions of AoI and PAoI are obtained for a single-source bufferless PH/PH/1/1 queue with probabilistic preemption and also a single packet buffer $M/PH/1/2$ queue when the packet in the waiting room is replaced by a new arriving fresh packet with an arbitrary probability [12]. Multi-source systems have also attracted the attention of researchers. The reference [13] studies a multi-source $M/M/1$ queue with FCFS, preemptive bufferless, and non-preemptive single buffer with replacement queuing disciplines, using Stochastic Hybrid Systems (SHS) and derive the mean AoI for each source. Moreover, the authors find the region of feasible average status ages for multiple updating sources and also characterize how a service facility can be shared among multiple sources. The reference [14] obtains the average PAoI for $M/G/1$ and $M/G/1/1$ systems with heterogeneous service time requirements. A two-source $M/M/1/2$ queuing system is studied using SHS techniques in [15] where a packet waiting in the queue is replaced by a newly arriving packet from the same source.

A number of research studies focus on discrete-time AoI queuing models. An FCFS-type $Ber/G/1$ queue is studied in [16] which derives explicit expressions for the average AoI and PAoI and also mean AoI expressions for the discrete-time LCFS queue. In [17], the authors investigate a single-source discrete-time system for FCFS, preemptive LCFS, and bufferless (with packet dropping) queuing schemes and they derive closed-form expressions for the generating functions and the stationary distributions of the AoI and the PAoI. In another recent work [18], the authors study a discrete-time multi-source system using QBD Markov chains and obtain the exact distributions of per-source AoI and PAoI for systems with non-preemptive bufferless, preemptive bufferless and non-preemptive single buffer with replacement queuing disciplines. Herein this paper, the current work is inspired by the proposed approach employed in [18] in the setting of a single-hop, coordinated access system model, in order to obtain the probability distributions of the AoI and PAoI sequences for a vastly different cooperative random access network involving two-hop multi-path communication and random access transmission.

Recently, there has been an increase of interest in AoI in multi-hop scenarios. The reference [19] investigates a general multi-hop network where packets of a source disperse through the network from an entry point. The authors show that if the transmission times of packets are exponentially distributed, among all possible scheduling policies of the nodes, the Last-Generated-First-Served preemptive policy minimizes the average age of the stream. The authors of [20] consider a time-slotted network scenario where a source node transmits the status updates to a

destination with the help of a relay node while the direct link also exists and the transmissions of source and relay nodes are scheduled. Two age-oriented relaying protocols are devised in this work to reduce the AoI at destination, and the closed-form average AoI is derived for both protocols. The reference [21] investigates a two-hop continuous-time system where status updates are captured by both nodes, however, higher priority is considered for the packets that travel through the two-hop link to destination. Exact distributions of AoI and PAoI are derived for the non-priority packets while tight bounds are found for the priority flow. In this paper, a two-hop network is studied in discrete-time for which transmissions of the source and relay nodes use random access which is a different scenario than the ones that are mentioned above.

AoI has also been studied for non-cooperative random access networks as well. The authors of [22] investigate a random access scenario where sources send their status updates to a destination using a variation of slotted Aloha and obtains the average AoI while comparing the proposed random access method with conventional slotted Aloha and round robin protocols. The reference [23] studies the impact of Irregular Repetition Slotted Aloha (IRSA) on AoI with IRSA being a modern random access protocol which has recently emerged as a promising solution to support massive machine-type communications. In [23], the steady state distribution of AoI and its expected value are derived in closed-form. The reference [24] proposes decentralized age-efficient transmission policies for random access channels with multiple transmitters and shows that the slotted Aloha-type algorithms are asymptotically age-optimal only when the arrival rates are less than a specified threshold. The authors of [25] present a steady-state analysis of threshold-Aloha which is a distributed age-aware extension of slotted Aloha. In threshold-Aloha, each node suspends its transmission until a certain age threshold is reached and then it attempts to transmit with a fixed probability. Also, the authors of [26] propose an age-oriented random access protocol for massive IoT networks whereas [27] studies AoI in random access networks with stochastic arrivals. AoI has also been studied in Carrier-Sense Multiple Access (CSMA) environments [28, 29]. In this paper, slotted Aloha is considered as the Medium Access Control (MAC) protocol because of its analytical tractability as well as the simplicity of its implementation.

3 QBD Markov chains

QBD Markov chains studied in the current paper are described based on [30]. The studied infinite QBD-type discrete-time Markov chain, denoted by Ξ , is a two-dimensional Markov chain $X_\ell = (L_\ell, P_\ell)$ where $L_\ell, 0 \leq L_\ell \leq$

∞ and P_ℓ represent the level sequence and the phase sequence, respectively, and Ξ has an irreducible and positive recurrent probability transition matrix P_Ξ in the following block tridiagonal form:

$$P_\Xi = \begin{bmatrix} A_{00} & A_{01} & & & & \\ A_{10} & C & D & & & \\ & B & C & D & & \\ & & & B & C & D \\ & & & & \ddots & \ddots & \ddots \end{bmatrix}, \tag{1}$$

where A_{00}, A_{01} , and A_{10} are non-negative matrices of sizes $a \times a, a \times b, b \times a$, respectively, and the matrices B, C , and D are of size $b \times b$. There is a stationary probability vector $\pi = [\pi_0 \ \pi_1 \ \dots]$ of this QBD where π_k is the solution vector for level k and is of size $1 \times a$ for $k = 0$ and $1 \times b$ for $k \geq 1$, and $\pi(k, \ell)$ denotes the ℓ th entry of π_k . In particular, the infinite row vector π satisfies the following equations uniquely:

$$\pi = \pi P_\Xi, \quad \pi_0 I_a + \sum_{k=1}^{\infty} \pi_k I_b = 1, \tag{2}$$

where I_l denotes a column vector of ones of size l . Additionally, π_k is in the following matrix-geometric form:

$$\pi_k = \pi_1 R^{k-1}, \quad k \geq 2, \tag{3}$$

with the rate matrix R being the solution of the following quadratic matrix equation

$$R = R^2 B + R C + D. \tag{4}$$

Hence, the computation of the rate matrix R is key to the steady-state solution of QBDs. The unique solution to the equation (4) can be obtained by existing computationally efficient solvers such as the ordered Schur decomposition based approach [31] or the logarithmic reduction procedure [32]. However, for the QBDs of interest to the current paper, the problem is even simpler since the matrix C will be shown to be all zeros and the matrices B and D will be shown to be in the following form:

$$B = \begin{bmatrix} \mathbf{0}_{(b-l) \times (b-l)} & \mathbf{0}_{(b-l) \times l} \\ \mathbf{0}_{l \times (b-l)} & I_l \end{bmatrix}, \quad D = \begin{bmatrix} D_0 & D_1 \\ \mathbf{0}_{l \times (b-l)} & \mathbf{0}_{l \times l} \end{bmatrix}, \tag{5}$$

for some matrices D_0, D_1 , and $l > 0$, where I_l denotes the identity matrix of size l and $\mathbf{0}_{b \times l}$ is an all-zeros matrix of size $b \times l$. In this case, the matrix R defined as

$$R = \begin{bmatrix} D_0 & -D_0^{-1} D_1 \\ \mathbf{0}_{l \times (b-l)} & I_l \end{bmatrix}, \tag{6}$$

can easily be shown to satisfy the equation (4).

Table 1 Possible events in the network and their probabilities

Event	Probability
Succ. ^a from S to D	$r_{S,D} \triangleq p_S(1 - p_R)\phi_{S,D}$
Succ. from S to R (if Q is full)	$r_{S,R} \triangleq p_S(1 - p_R)(1 - \phi_{S,D})\phi_{S,R}$
Succ. from S to R (if Q is empty)	$r_{S,R}\alpha$
Succ. from R (status update) to D (if Q is empty)	$r_{R,D} \triangleq p_R(1 - p_S)\phi_{R,D}$
Succ. from R (status update) to D (if Q is full)	$r_{R,D}(1 - \beta)$
Succ. from Q to D (if Q is full)	$r_{R,D}\beta$
Unsucc. ^b from S or R due to channel inefficiencies	$r_u \triangleq p_R(1 - p_S)(1 - \phi_{R,D}) + p_S(1 - p_R)(1 - \phi_{S,D})(1 - \phi_{S,R})$
No transmission (idle time slot)	$r_i \triangleq (1 - p_S)(1 - p_R)$
Collision	$r_c \triangleq p_S p_R$
Collision or unsucc. or idle	$r_0 \triangleq r_c + r_u + r_i$

^aSuccessful transmission^bUnsuccessful transmission

4 System model

In this paper, a slotted Aloha-based cooperative wireless network is investigated where two half duplex¹ nodes, namely the source node S and the relay node R, send status update packets of two underlying stochastic processes, namely the source and relay processes, respectively, to a common destination D. Moreover, R holds a so-called *relay queue* Q to buffer the unsuccessfully transmitted packets of S for further re-transmissions. Q is assumed to be a single buffer queue which holds the last accepted packet of S. Figure 1 depicts the described network. Due to the random access mechanism, collision (simultaneous transmissions of more than one node) may occur in which case D is not able to decode any of the transmitted packets. The physical layer considerations (e.g., channel fading characteristics or applied diversity and coding methods), are modeled by the success probability $\phi_{u,v}$ for transmission from node u to node v (link $u-v$), where $u \in \{S, R\}$ and $v \in \{R, D\}$. Each status update is generated at the onset of the time slot it is transmitted. Thus, status updates do not wait at the nodes before they are transmitted.

At the beginning of each time slot, a status update of the source process is generated and transmitted by S with transmission probability p_S . The transmitted packet is successfully delivered to D unless it is erased either due to channel errors (with the probability $1 - \phi_{S,D}$) or due to collision. Upon successful transmission, an ACK message from D informs R of the successful transmission to drop the potential existing packet in Q. Note that, since the successfully transmitted packet via the direct link S-D is

fresher than the waiting packet in Q, there is no benefit in holding the packet in Q any more, thus R should drop it upon hearing an ACK from D. However, in case of unsuccessful transmission on the direct link, R may also be able to decode the packet with probability $\phi_{S,R}$ provided that there is no collision. The ACK messages are assumed to be immediately heard by both source and relay nodes with no errors. Herein this paper, R adopts an admission controlled replacement policy as follows: Once a packet of S is received at R, it replaces the existing staler packet in Q provided there is any. However, if Q is empty, then the new packet is accepted with the so-called *acceptance probability* α . On the other hand, if R decides to send a packet with transmission probability p_R at the onset of a time slot, it should decide whether to transmit a newly generated status update of the relay process (its own packet) or the existing packet in Q (if any). Once Q is empty, R sends its own fresh packet. Otherwise, R transmits the waiting packet in Q with the so-called *relay probability* β , or its own packet with probability $1 - \beta$. Either way, the transmitted packet is received successfully at D with the success probability $\phi_{R,D}$ unless it has collided. If the relayed packet of S is received successfully at D, an ACK from D informs R to drop that packet from Q. Accordingly, the transmission procedure at each time slot in S is simply to decide whether to transmit a packet based on the transmission probability p_S . On the other hand, the transmission procedure in R is described in Algorithm 1, in which the notation ‘w.p.’ stands for ‘with probability’. Also, according to the described scenario, Table 1 provides the probabilities of all possible events in the network.

It is worth noting that R adopts two probabilistic cooperation control mechanisms: admission control when

¹ Full duplex capability can also be considered for nodes as in [5].

Q is empty and relaying control when it is full. Similar cooperation mechanisms have been considered in [5, 8]. In fact, having two degrees of freedom, i.e., α and β , instead of just one (α or β), is especially useful when some additional constraints should be met in the network. For example, as illustrated in Sect. 6, considering both parameters α and β works more efficiently than just using β , when the PAoI of R is constrained. For convenience, the specific choice of the pair (α, β) is referred to as the *cooperation policy* of R. In a non-cooperative network, R adopts the no-cooperation policy, i.e., $\alpha = 0$ (or $\beta = 0$). On the other hand, in the full-cooperative network, R accepts

all the incoming packets from S and prioritizes them over its own packets upon making transmission decisions, i.e., $\alpha = \beta = 1$.

Let the discrete-time discrete-valued random sequence $\Delta_u(\ell)$ denote the AoI governed by the status update packets transmitted by node u ($u \in \{S, R\}$), monitored by D at time slot ℓ . By definition, $\Delta_u(\ell) = \ell - \delta_u(\ell)$ where $\delta_u(\ell)$ is the instance of generation of the most recent received packet of u at D. More specifically, suppose that the j th successful packet of node u is generated at time slot δ_u^j and received successfully at D at time slot θ_u^j . Then, $\Delta_u(\ell)$ starts from $\Delta_u(\theta_u^j) = \theta_u^j - \delta_u^j$ and increases monotonically in time until

Algorithm 1 Transmission Procedure of the Relay Node at each Time Slot

```

1: Decide whether to transmit a packet based on the probability  $p_R$ .
2: if transmission decision is to transmit then
3:   if Q is empty then
4:     Generate and transmit a new packet of its own.
5:   else
6:     Choose between Q (w.p.  $\beta$ ) and its own packet (w.p.  $1 - \beta$ ).
7:     if Q is chosen then
8:       Transmit the packet in Q.
9:       Wait for the acknowledgement message from D.
10:      if ACK is received from D then
11:        Drop the packet from Q.
12:      else
13:        Keep the packet in Q.
14:      end if
15:    else if
16:      Generate and transmit a new packet of its own.
17:    end if
18:  end if
19: else
20:   if a new packet of S is decoded then
21:     Wait for an acknowledgement message from D destined to S.
22:     if ACK is received from D then
23:       Drop the new packet.
24:       Drop the possibly existing packet in Q.
25:     else
26:       Keep the packet in Q (replace its existing packet, if any).
27:     end if
28:   end if
29: end if

```

the next packet of u is delivered successfully to D, i.e., time slot θ_u^{j+1} . At that time, $\Delta_u(\ell)$ suddenly drops to $\theta_u^{j+1} - \delta_u^{j+1}$. At the instance just before the $(j + 1)$ th packet is received, age of the j th packet takes the maximum value, namely $\theta_u^{j+1} - \delta_u^j$, which is called the peak age of the j th packet. The sequence $\Lambda_u(\ell)$, known as the *peak AoI* of packets of node u , is the sequence obtained by concatenating these peak values. Figure 2 depicts a sample path of $\Delta_u(\ell)$ and $\Lambda_u(\ell)$. Note that, since each packet takes at least one time slot to be received successfully at D, $\Delta_u(\ell)$ takes the minimum value 1. Consider the j th packet of node u which is aged at D from time slot θ_u^j to $\theta_u^{j+1} - 1$. The sub-sequence of $\Delta_u(\ell)$ where $\ell \in [\theta_u^j, \theta_u^{j+1} - 1]$ is referred to as the *age cycle* of successful packet j of node u . Therefore, $\Delta_u(\ell)$ is simply composed of successive age cycles of successively received packets of node u at D.

The notations Δ_u and Λ_u are used to denote the steady state random variables associated with the sequences $\Delta_u(\ell)$ and $\Lambda_u(\ell)$, respectively, where their steady state probability mass functions (pmf) are denoted by $p_{\Delta_u}(n)$ and $p_{\Lambda_u}(n)$:

$$p_{\Delta_u}(n) = \lim_{\ell \rightarrow \infty} \Pr(\Delta_u(\ell) = n), \quad n \geq 1, \tag{7}$$

$$p_{\Lambda_u}(n) = \lim_{\ell \rightarrow \infty} \Pr(\Lambda_u(\ell) = n), \quad n \geq 1, \tag{8}$$

where $\Pr(\cdot)$ denotes the probability of its argument.

5 Distribution of the AoI and PAoI sequences

A similar approach to [18] is followed here to obtain the pmfs $p_{\Delta_u}(n)$ and $p_{\Lambda_u}(n)$ ($u \in \{S, R\}$) by modeling the journey of each packet (originated by node u) from the instance of its generation and then its successful transmission to D (the beginning of the age cycle of the packet), till the instant at which the next packet is received successfully at D (when the age cycle ends), by a QBD Markov chain $X_\ell = (L_\ell, P_\ell), \ell = 1, 2, \dots$, which was briefly described in Sect. 2. Let's denote the packet of interest, whose journey is being modeled, by P_0 . The phases of the QBD X_ℓ represent the state of the system regarding P_0 , while the levels, starting from level 1, model the elapsed time since the generation of P_0 . More specifically, once P_0 is generated and transmitted successfully to another node, i.e., D or Q (for the packets of S), its journey starts at level 1. Following that, the QBD's level increases by 1 after each time slot, until the next packet of node u is received successfully at D, that is when the age cycle of P_0 ends and the QBD should be restarted from level 1 to account for the journey of another packet. To maintain the QBD form of the Markov chain, certain *auxiliary phases*

are used for restarting the QBD from level 1. These phases are described where the QBD models are detailed.

5.1 QBD model for the relay node

Once a packet of R (e.g., P_0) is generated at the beginning of a time slot and delivered to D at the end of that time slot, its journey in the proposed QBD (named Ξ_R , depicted in Fig. 3) begins from level 1 at phase E or F, depending on whether Q is empty or full at that time, respectively. Following that, till the next successful transmission from R to D, the state of Q may change due to transmissions from S or Q, hence the phase of Ξ_R may change between E or F in successive levels. When the next packet of R is delivered to D, the age cycle of P_0 ends and Ξ_R should be restarted from level 1, to account for the age cycle of the next packet of R. To this end, the auxiliary phases T_e and T_f are introduced to go back (level by level) from phases E and F, respectively. Note that if the new packet arrives at D when Q is empty (or full), Ξ_R should be restarted at phase E (F, resp.). Transition probabilities are detailed in Fig. 3. Recalling the definition of $\Delta_R(n)$ and $\Lambda_R(n)$, the phases K_e and K_f are introduced in Ξ_R to find $p_{\Lambda_R}(n)$. In fact, these states indicate the maximum value of age of P_0 just before resetting to 1 (due to the new packet arrival). Thus, $p_{\Lambda_R}(n)$ can be written as

$$p_{\Lambda_R}(n) = \lim_{\ell \rightarrow \infty} \Pr(L_\ell = n \mid P_\ell \in \{K_e, K_f\}), \tag{9}$$

$$= \frac{\pi_r(n, K_e) + \pi_r(n, K_f)}{\sum_{m=1}^{\infty} (\pi_r(m, K_e) + \pi_r(m, K_f))}, \tag{10}$$

where $\pi_r(x)$ is the steady state probability of being in joint state x of the QBD Ξ_R . Note that the auxiliary phases T_e and T_f are only introduced to restart Ξ_R , and also the phases K_e and K_f to calculate $p_{\Delta_R}(n)$. Henceforth, $p_{\Delta_R}(n)$ can be written as:

$$p_{\Delta_R}(n) = \lim_{\ell \rightarrow \infty} \Pr(L_\ell = n \mid P_\ell \in \{E, F\}), \tag{11}$$

$$= \frac{\pi_r(n, E) + \pi_r(n, F)}{\sum_{m=1}^{\infty} (\pi_r(m, E) + \pi_r(m, F))}. \tag{12}$$

5.2 QBD model for the source node

Studying $\Delta_S(n)$ is different from $\Delta_R(n)$ as packets of S reach D via two links: the direct and relay links. Age cycle of the packets that traverse the direct link, starts from 1, while the packets that travel through the relay link wait at Q for some time slots before they are delivered to D, provided that they are not replaced or dropped. Hence, the age cycle of the packet that passes the relay link, if not replaced or dropped, starts from a value larger than 1 (at

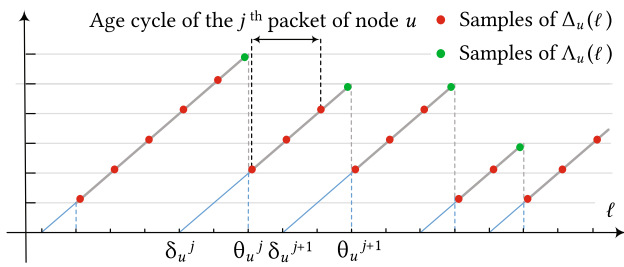


Fig. 2 Sample path of the AoI and PAoI sequences of node u

least 2, due to 1 time slot for S to R and 1 time slot for Q to D transmissions). Therefore, in the proposed QBD (named Ξ_S , refer to Fig. 4) that models the journey of packets of S (e.g., P_0) in the network, the phase W is introduced to track the packets who travel through the relay link. Thus, once P_0 is accepted at Q, its journey in Ξ_S starts from state W at level 1. If the packet is replaced or dropped, Ξ_S is tracking a faulty packet, as age is not defined for a packet which is not received at D. In that case, Ξ_S should start over at level 1, tracking the newly received packet at R (that replaced P_0) or D (which forced R to drop P_0), which is done by the auxiliary phases T_p and T_d , respectively. On the other hand, if P_0 is not replaced or dropped, it is relayed to D by R at some time slot.

Once P_0 is received at D, via either direct or relay links, its age cycle starts and the level in Ξ_S increases by time until the next packet of S is successfully received at D. During this time, other packets of S may be accepted at Q and change the phase of Ξ_S from E to F (recall that once P_0 is received at D, Q becomes empty). Upon arrival of a new packet of S to D, by using the auxiliary phase T, Ξ_S restarts from level 1 to track the new packet.

Note that each packet of S may find Q empty or full when it departs S. If Q is full and the new packet of S drops or replaces the existing packet in Q, the phases T_d and T_p restart Ξ_S so that it models the journey of the new packet. Thus, when Ξ_S is restarted by means of phase T, it is going to track the journey of a packet which has entered the network when Q is empty. In that case, the packet enters R or D, respectively, by probabilities

$$\eta_w^e \triangleq \frac{r_{S,R}\alpha}{(r_{S,D} + r_{S,R}\alpha)}, \quad \eta_e^e \triangleq \frac{r_{S,D}}{(r_{S,D} + r_{S,R}\alpha)}, \quad (13)$$

where $r_{S,D} + r_{S,R}\alpha$ is the probability of a successful transmission from S (to R or D), provided that Q is empty. Also, by using the same reasoning as in Sect. 5.1, the phase K is introduced to Ξ_S to find $p_{\Lambda_S}(n)$ as

$$p_{\Lambda_S}(n) = \lim_{\ell \rightarrow \infty} \Pr(L_\ell = n | P_\ell = K), \quad (14)$$

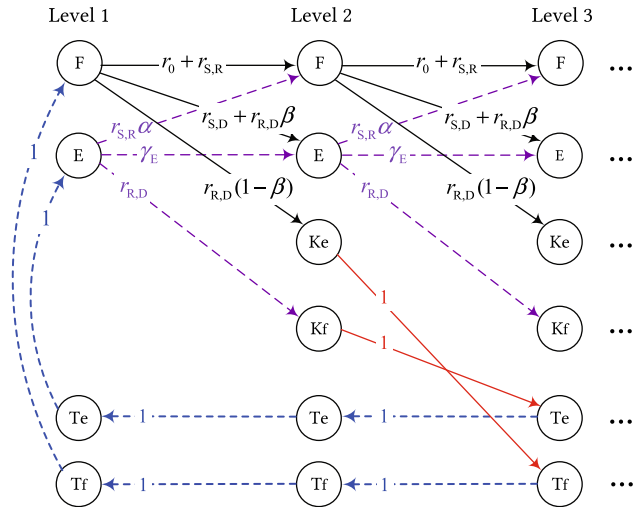


Fig. 3 The transition diagram of Ξ_R , where $\gamma_e \triangleq r_0 + r_{S,D} + r_{S,R}(1 - \alpha)$

$$= \frac{\pi_S(n, K)}{\sum_{m=1}^{\infty} \pi_S(m, K)}, \quad (15)$$

where $\pi_S(x)$ is the steady state probability of being in joint state x of the QBD Ξ_S . Note that the auxiliary phases just aim to maintain the QBD structure of Ξ_S while restarting, also the goal of phase K is to find $p_{\Lambda_S}(n)$ and the phase W tracks the packets whose age cycle has not yet begun. Thus, $p_{\Lambda_S}(n)$ can be written as:

$$p_{\Lambda_S}(n) = \lim_{\ell \rightarrow \infty} \Pr(L_\ell = n | P_\ell \in \{E, F\}), \quad (16)$$

$$= \frac{\pi_S(n, E) + \pi_S(n, F)}{\sum_{m=1}^{\infty} (\pi_S(m, E) + \pi_S(m, F))}. \quad (17)$$

6 Numerical results

6.1 Model validation using simulations

In this subsection, the proposed analytical model is verified by using simulations. To that end, the marginal pmfs of the AoI and PAoI sequences of S and R are obtained using the proposed analytical model, and the results are confirmed by numerous simulations. Figure 5 depicts the marginal pmf of AoI of both nodes for two different values of $\phi_{S,D}$ while fixing $\alpha = \beta = 0.5$, $\phi_{R,D} = 0.9$ and $\phi_{S,R} = 1$ with the two choices of transmission probabilities $p_S = p_R = 0.65$ and $p_S = 0.25, p_R = 0.65$. Also, the pmfs of the PAoI sequences of the source and relay nodes are depicted in Fig. 6. Note that, in general, the assignment of numerical values to the related parameters is arbitrary, however, the

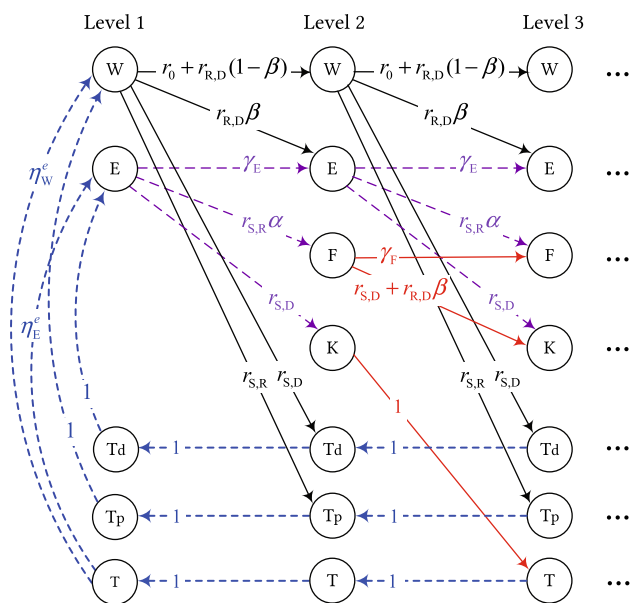


Fig. 4 The transition diagram of Ξ_S , where $\gamma_E \triangleq r_0 + r_{R,D} + r_{S,R}(1 - \alpha)$ and $\gamma_F \triangleq r_0 + r_{S,R} + r_{R,D}(1 - \beta)$

assignments $\phi_{R,D} = 0.9$, $\phi_{S,R} = 1$ and $p_S = p_R = 0.65$ are chosen to be consistent with the following sections in which a search space is to be explored in certain optimization attempts. Also, the assignment $p_S = 0.25, p_R = 0.65$ is chosen such that the curves in Fig. 5 (as well as in Fig. 6) be distinguishable. As observed, the obtained results using the proposed analytical model match perfectly with the simulation results, which are indicated by A (Analysis) and S (Simulation), respectively, in the legends.

6.2 Weighted-sum-average of the source and relay AoI sequences

Weighted-Sum-Average (WSA) of the AoI sequences of the source and relay nodes is defined as

$$WSA = \omega_S E[\Delta_S] + \omega_R E[\Delta_R], \tag{18}$$

where ω_S and ω_R are real-valued non-negative normalized weights, i.e., $\omega_S + \omega_R = 1$, associated with S and R, and $E[\cdot]$ indicates the expectation operator. Being a commonly used performance metric, WSA can be obtained readily by using the marginal distributions of the associated AoI sequences in Sect. 5.

In Sect. 6.2.1, assuming fixed values for transmission probabilities of S and R, i.e., p_S and p_R , the optimal cooperation policy is found (determined by optimal values of α and β), which minimizes the WSA, constrained to limited deviation in $E[\Lambda_R]$. Then, in Sect. 6.2.2, the optimal values of transmission probabilities as well as the optimal cooperation policy (forming optimization with

respect to the variables p_S, p_R, α and β) are explored aiming to minimize the unconstrained WSA.

6.2.1 Optimal cooperation policy for fixed transmission probabilities

In this subsection, the following problem is addressed:

$$\underset{\alpha, \beta}{\text{minimize}} \quad \omega_S E[\Delta_S] + \omega_R E[\Delta_R] \tag{19a}$$

$$\text{subject to} \quad E[\Lambda_R] \leq (1 + h_R) E[\Lambda_R^{NC}] \tag{19b}$$

$$0 \leq \alpha, \beta \leq 1, \tag{19c}$$

where Λ_R^{NC} denotes Λ_R in the non-cooperative network and the non-negative parameter h_R determines the maximum allowed increase in $E[\Lambda_R]$ with respect to $E[\Lambda_R^{NC}]$. Note that, in the non-cooperative network, R does not devote any resources to relay the packets of S, therefore, $E[\Lambda_R]$ is minimized.

Using exhaustive search, where α and β change from 0 to 1 by the step size 0.001, and by exploiting the QBD-based analytical model, the WSA-optimal cooperation policy has been obtained in various scenarios. More specifically, we have considered good and mediocre R-D channel states, i.e., $\phi_{R,D} = 0.9$ and 0.6, respectively, and also perfect and medium states for the S-R channel, i.e., $\phi_{S,R} = 1$ and 0.5, respectively, while $\phi_{S,D}$ is varied from 0.2 to 0.7. Also, different relative weights have been considered for the nodes S and R, indicated by $\omega = 1/3, 1, 3$ ($\omega \triangleq \omega_R / \omega_S$). In addition, the results are obtained where $E[\Lambda_R]$ is tightly and loosely constrained, i.e., $h_R = 0.1$ and 1, respectively. Nodes' transmission probabilities are fixed to $p_S = p_R = 0.65$ in this example, however their optimal values are sought in Sect. 6.2.2.

Figure 7 compares WSA in a network powered by the WSA-optimal policy and the non-cooperative network. As observed, WSA is significantly reduced when the optimal policy is applied which is due to the cooperation aspect of the system as well as the employment of the optimal policy. The improvement can be up to 53% especially in network scenarios with poor S-D channels. As illustrated in Fig. 8, the optimal policy also outperforms the full-cooperation policy for more than 33% in poor S-D channels. Figures 7 and 8 reveal that not only cooperation helps improve the WSA performance, but also the optimal choices of α and β can further reduce it substantially.

In fact, in the full-cooperation policy, the AoI of S is minimized, however, packets of R have the least priority and experience the longest inter-departure time. On the other hand, in the non-cooperative network, R devotes all of its resources to send its own packets, hence, AoI of S is maximized unlike AoI of R. However, in the optimal

Fig. 5 Pmf of the source and relay AoI sequences for two values of $\phi_{S,D}$ when $\phi_{R,D} = 0.9$, $\phi_{S,R} = 1$ and $\alpha = \beta = 0.5$, for the cases $p_S = p_R = 0.65$ and $p_S = 0.25, p_R = 0.65$

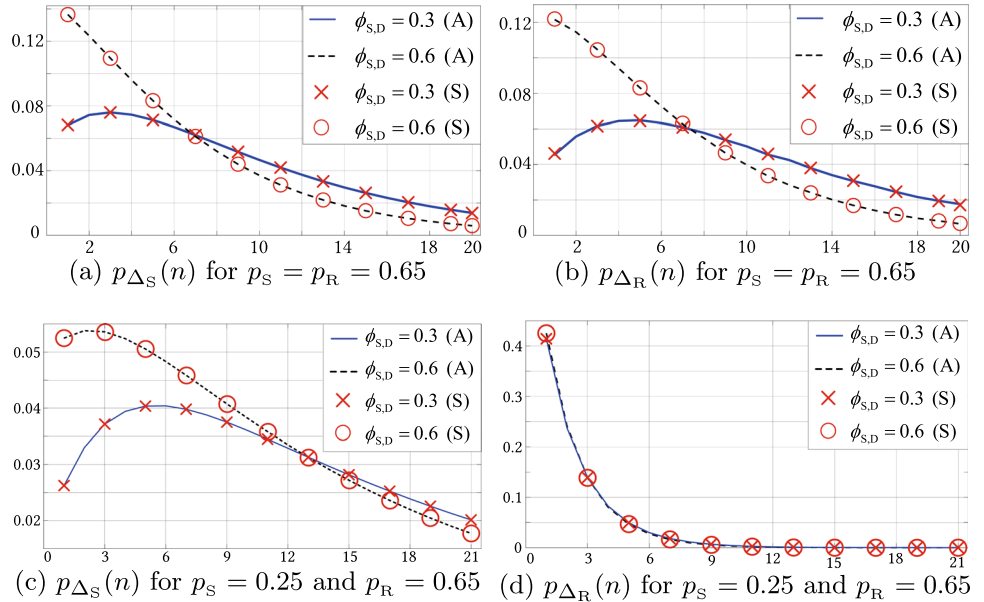
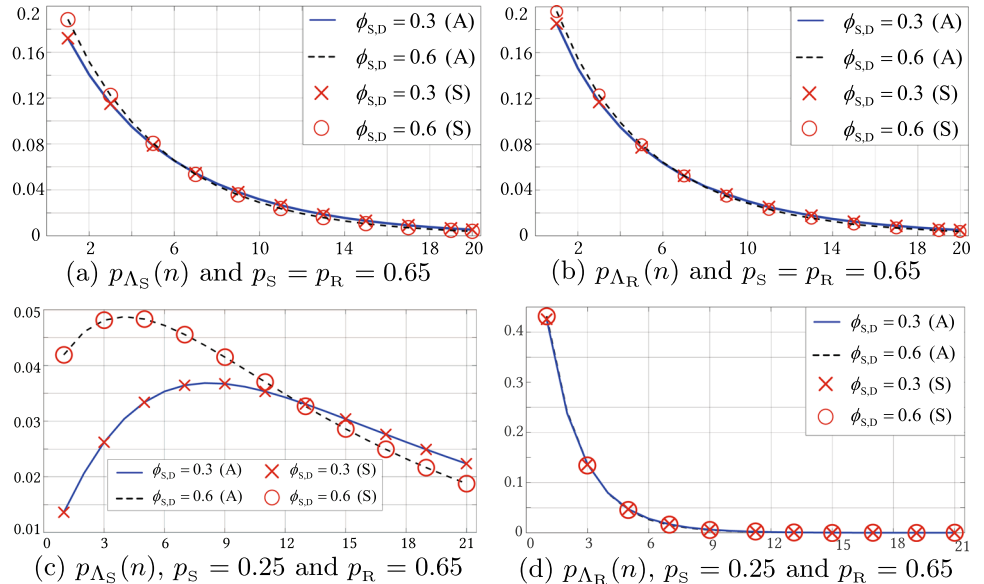


Fig. 6 Pmf of the source and relay PAoI sequences for two values of $\phi_{S,D}$ when $\phi_{R,D} = 0.9$, $\phi_{S,R} = 1$ and $\alpha = \beta = 0.5$, for the cases $p_S = p_R = 0.65$ and $p_S = 0.25, p_R = 0.65$



policy, R adjusts α and β such that AoI of the nodes is closest to each other in a way that the corresponding WSA is minimized. Note that from a different point of view, devoting time to relay all the incoming packets of S in the full-cooperative network, causes that in some cases $E[\Lambda_R]$ exceeds the desired threshold, particularly when it is tightly constrained. In Fig. 8(b), only the scenarios where the constraint is satisfied have been considered. More specifically, the full-cooperative policy does not satisfy the constraint on $E[\Lambda_R]$ with $h_R = 0.1$ in network scenarios where $\omega = 1/3$ and $\phi_{R,D} = 0.9$ for any assessed S-D channel status and also in some other studied cases in Fig. 8(b).

6.2.2 Joint optimization of transmission probabilities and cooperation policy

In this subsection, WSA is minimized with respect to the transmission probabilities as well as the acceptance and relaying probabilities. Mathematically, the following optimization problem is investigated:

$$\underset{\alpha, \beta, p_S, p_R}{\text{minimize}} \quad \omega_S E[\Delta_S] + \omega_R E[\Delta_R] \tag{20a}$$

$$\text{subject to} \quad 0 \leq \alpha, \beta, p_S, p_R \leq 1. \tag{20b}$$

For the sake of convenience, we have removed the constraint on $E[\Lambda_R]$ for this problem. The resultant optimal transmission and cooperation policy is referred to as the

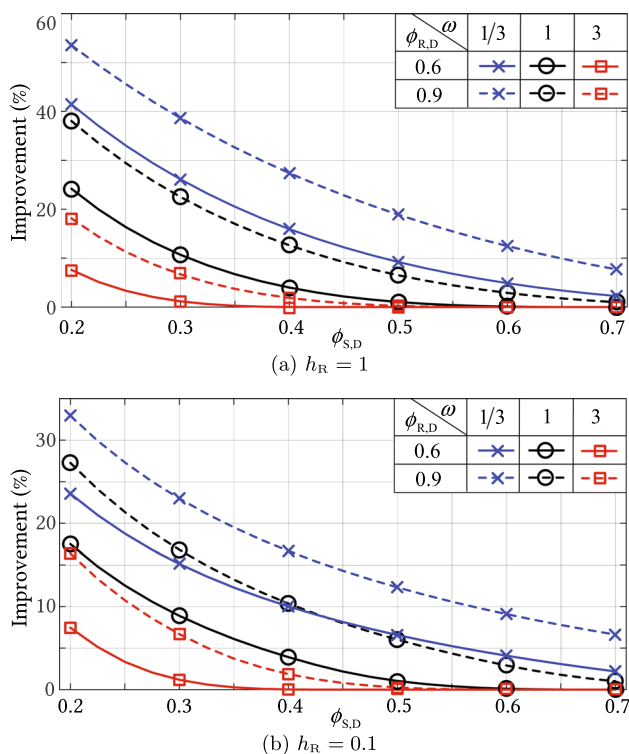


Fig. 7 Percentage improvement in WSA performance gained by using the optimal cooperative policy with respect to the non-cooperation policy, for **a** $h_R = 1$ and **b** $h_R = 0.1$, where $p_S = p_R = 0.65$, $\phi_{R,D} = 0.6, 0.9$, $\phi_{S,R} = 1$ and $\omega = 1/3, 1, 3$

overall-optimal policy. Using exhaustive search where p_S and p_R are varied from 0.05 to 0.95 with step size being 0.1, and also α and β are varied from 0 to 1 with steps of size 0.001, the optimal transmission probabilities and cooperation parameters are obtained for $\phi_{R,D} = 0.9$, $\phi_{S,R} = 1, 0.5$ while $\phi_{S,D}$ is varied from 0.2 to 0.7.

Figure 9 illustrates the obtained optimal values of p_S and p_R , denoted by p_S^{opt} and p_R^{opt} . As seen, transmitting at very low or high probabilities degrades the performance in the sense of (20a), more specifically, $0.35 \leq p_S^{opt}, p_R^{opt} \leq 0.65$ in the explored numerical examples. Also, employing equal values for p_S and p_R is not the optimal choice in most of cases. On the contrary, especially when AoI of S and R are not equally weighted, p_S^{opt} and p_R^{opt} can be significantly far from each other. Moreover, relative values of p_S^{opt} and p_R^{opt} depend highly on the parameter ω , meaning that, for $\omega > 1$, i.e., $\omega_R > \omega_S$, $p_R^{opt} > p_S^{opt}$ and vice versa, in most cases. Another observation comparing Fig. 9(a) and (b) is that, the state of the S-R channel does not affect p_S^{opt} and p_R^{opt} very much, at least within the numerical settings of the current study. However, degraded S-R channel may result in higher values of p_S^{opt} to compensate for the inefficiencies in this channel.

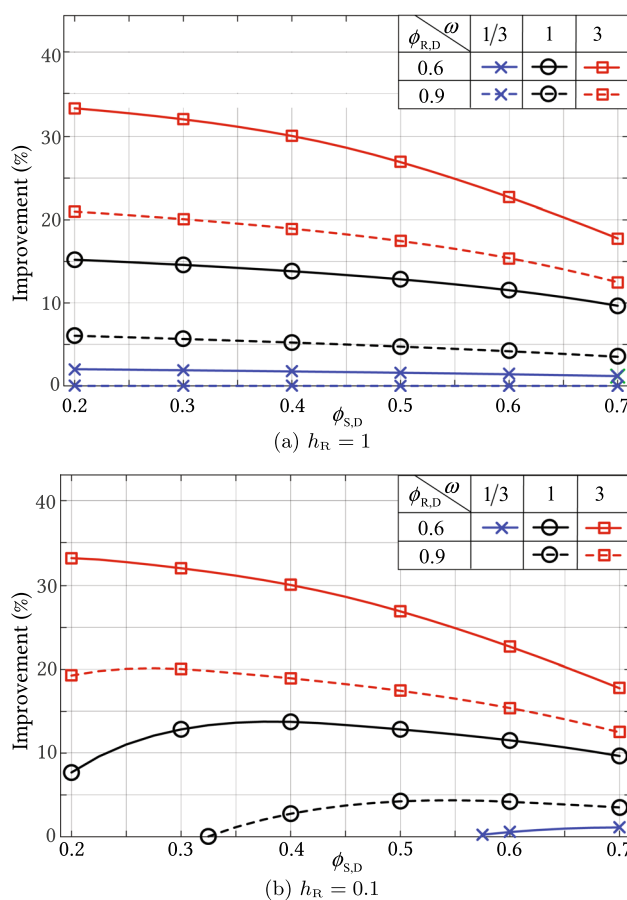


Fig. 8 Percentage improvement in WSA performance gained by using the optimal cooperative policy with respect to the full-cooperation policy, for **a** $h_R = 1$ and **b** $h_R = 0.1$, where $p_S = p_R = 0.65$, $\phi_{R,D} = 0.6, 0.9$, $\phi_{S,R} = 1$ and $\omega = 1/3, 1, 3$

Figure 10 depicts the percentage increase in WSA when the optimal cooperative policy with given transmission probabilities ($p_S = p_R = 0.65$ and 0.45) is applied compared to the overall-optimal policy. As observed, transmitting with non-optimal transmission probabilities can degrade performance in terms of WSA up to more than 40% for the choice of $p_S = p_R = 0.65$ and 25% when $p_S = p_R = 0.45$ (in the numerical settings here), especially when the S-D channel is downgraded and AoI of R is prioritized over AoI of S, i.e., $\omega = 3$. Figure 10 shows that choice of mediocre values for p_S and p_R , i.e., 0.45, results in less increase in WSA (which has been concluded from Fig. 9 earlier).

7 Conclusions

In this paper, we investigate a slotted Aloha-based cooperative status update network involving a source and a relay node. Exact marginal pmfs of AoI and also PAoI sequences of both nodes are obtained using QBD Markov

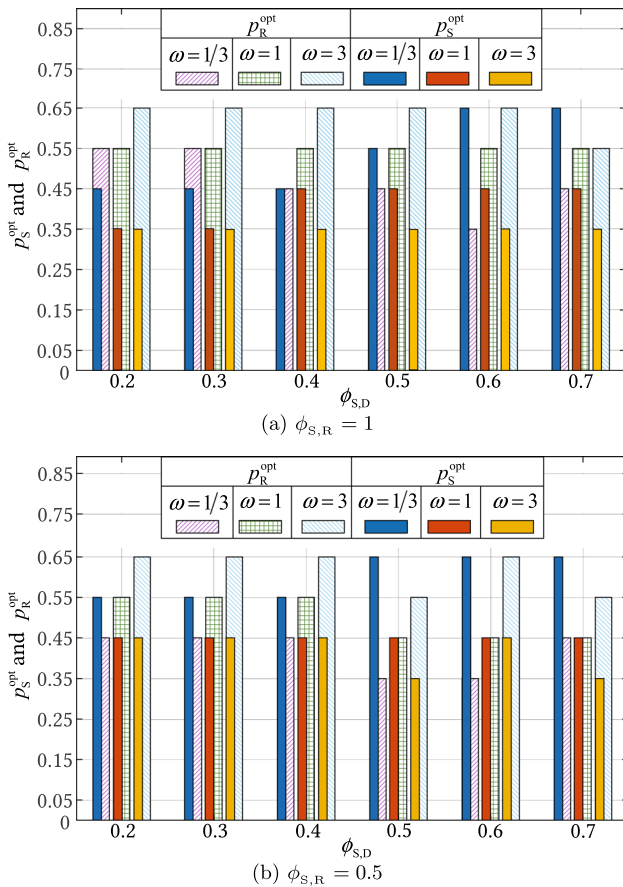


Fig. 9 Optimal values of p_S and p_R in the overall-optimal policy for different states of the S-D channel, where $\phi_{R,D} = 0.9$, $\omega = 1/3, 1, 3$ and $\phi_{S,R} = 0.5, 1$

chains and the proposed analytical model is validated by simulations. Subsequently, using the analytical model, the weighted-sum-average of the AoI sequences of the source and relay nodes is studied, which is termed as WSA in this paper. More specifically, certain optimum cooperation policies (defined by acceptance and relaying probabilities) are obtained. As observed, the optimal cooperation policy reduces WSA substantially with respect to the full-cooperative and non-cooperative policies. Moreover, thanks to the efficiency of the analytical model, the overall-optimal policies have been obtained by which the optimal values of the acceptance and relaying probabilities as well as the transmission probabilities are found by brute-force search. As observed, the optimal choice of the transmission probabilities and the acceptance and relaying probabilities can be very influential in terms of the minimization of WSA. Future work will involve the extension of the proposed models to more than two nodes as well as the joint distribution of the AoI and PAoI sequences of these nodes.

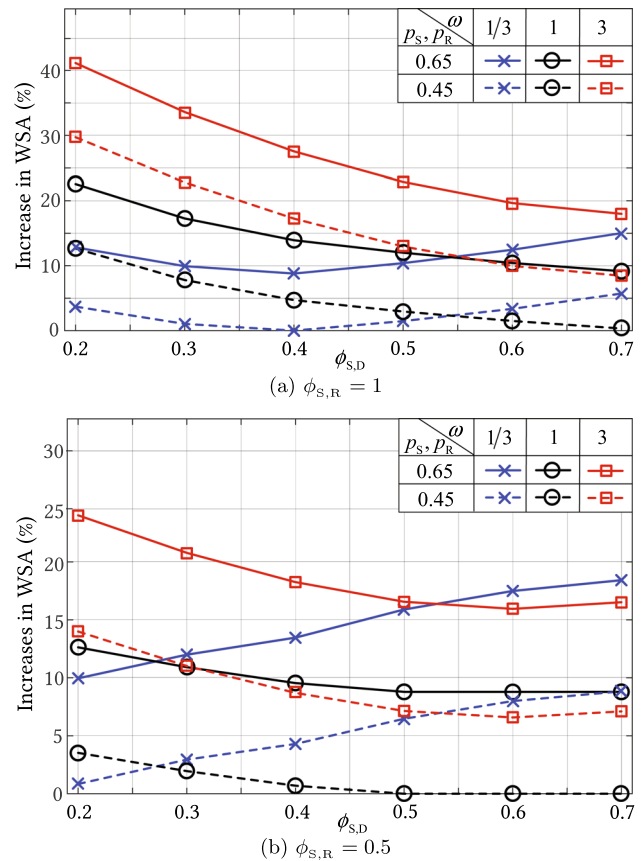


Fig. 10 Percentage increase in WSA by means of using the optimal cooperation policy with $p_S = p_R = 0.65$ as well as $p_S = p_R = 0.45$, compared to the overall-optimal policy, where $\phi_{R,D} = 0.9$, $\omega = 1/3, 1, 3$ and $\phi_{S,R} = 0.5, 1$

Data Availability The datasets generated and/or analysed during the current study are available from the corresponding author on reasonable request.

References

1. Kaul, S., Yates, R., & Gruteser, M. (2012). Real-time status: How often should one update? In *Proceedings IEEE INFOCOM* (pp. 2731–2735). <https://doi.org/10.1109/INFOCOM.2012.6195689>
2. Costa, M., Codreanu, M., & Ephremides, A. (2014). Age of information with packet management. In *IEEE ISIT* (pp. 1583–1587). <https://doi.org/10.1109/ISIT.2014.6875100>
3. Yates, R. D., Sun, Y., Brown, D. R., Kaul, S. K., Modiano, E., & Ulukus, S. (2021). Age of information: An introduction and survey. *IEEE JSAC*, 39(5), 1183–1210. <https://doi.org/10.1109/JSAC.2021.3065072>
4. Kosta, A., Pappas, N., & Angelakis, V. (2017). Age of information: A new concept, metric, and tool. *Foundations and Trends® in Networking®* 12(3), 162–259. <https://doi.org/10.1561/13000000060>
5. Vaezi, K., & Ashtiani, F. (2020). Delay-optimal cooperation policy in a slotted Aloha full-duplex wireless network: Static approach. *IEEE Systems Journal*, 14(2), 2257–2268. <https://doi.org/10.1109/JSYST.2019.2940605>

6. Li, B., Chen, H., Zhou, Y., & Li, Y (2020). Age-oriented opportunistic relaying in cooperative status update systems with stochastic arrivals. In *IEEE conference on GLOBECOM* (pp. 1–6). <https://doi.org/10.1109/GLOBECOM42002.2020.9321986>
7. Moradian, M., & Dadlani, A. (2020). Age of information in scheduled wireless relay networks. In *IEEE wireless communications and networking conference WCNC* (pp. 1–6). <https://doi.org/10.1109/WCNC45663.2020.9120608>
8. Vaezi, K., & Ashtiani, F. (2018). Delay-optimal static relaying policy in a slotted Aloha wireless network. In *Iran workshop on communication and information theory (IWCIT)* (pp. 1–6). <https://doi.org/10.1109/IWCIT.2018.8405045>
9. Kaul, S., Gruteser, M., Rai, V., & Kenney, J. (2011). Minimizing age of information in vehicular networks. In *8th annual IEEE communications society conference on sensor, mesh and ad hoc communications and networks* (pp. 350–358). <https://doi.org/10.1109/SAHCN.2011.5984917>
10. Costa, M., Codreanu, M., & Ephremides, A. (2016). On the age of information in status update systems with packet management. *IEEE Transactions on Information Theory*, 62(4), 1897–1910. <https://doi.org/10.1109/TIT.2016.2533395>
11. Inoue, Y., Masuyama, H., Takine, T., & Tanaka, T. (2019). A general formula for the stationary distribution of the age of information and its application to single-server queues. *IEEE Transactions on Information Theory*, 65(12), 8305–8324. <https://doi.org/10.1109/TIT.2019.2938171>
12. Akar, N., Doğan, O., & Atay, E. U. (2020). Finding the exact distribution of (peak) age of information for queues of PH/PH/1/1 and M/PH/1/2 type. *IEEE Transactions on Communications*, 68(9), 5661–5672. <https://doi.org/10.1109/TCOMM.2020.3002994>
13. Yates, R. D., & Kaul, S. K. (2019). The age of information: Real-time status updating by multiple sources. *IEEE Transactions on Information Theory*, 65(3), 1807–1827. <https://doi.org/10.1109/TIT.2018.2871079>
14. Huang, L., & Modiano, E. (2015). Optimizing age-of-information in a multi-class queueing system. In: *IEEE international symposium on information theory ISIT* (pp. 1681–1685). <https://doi.org/10.1109/ISIT.2015.7282742>
15. Moltafet, M., Leinonen, M., & Codreanu, M. (2020). Average age of information for a multi-source M/M/1 queueing model with packet management. In: *IEEE international symposium on information theory ISIT* (pp. 1765–1769). <https://doi.org/10.1109/ISIT44484.2020.9174099>
16. Tripathi, V., Talak, R., & Modiano, E. H. (2019). Age of information for discrete time queues. CoRR [arXiv:1901.10463](https://arxiv.org/abs/1901.10463)
17. Kosta, A., Pappas, N., Ephremides, A., & Angelakis, V. (2021). The age of information in a discrete time queue: Stationary distribution and non-linear age mean analysis. *IEEE Journal on Selected Areas in Communications*, 39(5), 1352–1364. <https://doi.org/10.1109/JSAC.2021.3065045>
18. Akar, N., & Doğan, O. (2021). Discrete-time queueing model of age of information with multiple information sources. *IEEE internet of things journal*. <https://doi.org/10.1109/JIOT.2021.3053768>
19. Bedewy, A. M., Sun, Y., & Shroff, N. B. (2017). Age-optimal information updates in multihop networks. In *IEEE international symposium on information theory (ISIT)* (pp. 576–580). <https://doi.org/10.1109/ISIT.2017.8006593>
20. Li, B., Wang, Q., Chen, H., Zhou, Y., & Li, Y. (2021). Optimizing information freshness for cooperative IoT systems with stochastic arrivals. *IEEE Internet of Things Journal*. <https://doi.org/10.1109/JIOT.2021.3051417>
21. Vikhrova, O., Chiariotti, F., Soret, B., Araniti, G., Molinaro, A., & Popovski, P. (2020). Age of information in multi-hop networks with priorities. In *IEEE global communications conference (GLOBECOM)* (pp. 1–6). <https://doi.org/10.1109/GLOBECOM42002.2020.9348175>
22. Atabay, D. C., Uysal, E., & Kaya, O. (2020). Improving age of information in random access channels. In *IEEE conference on computer communications workshops (INFOCOM WKSHPs)* (pp. 912–917). <https://doi.org/10.1109/INFOCOMWKSHPs50562.2020.9163053>
23. Munari, A. (2021). Modern random access: An age of information perspective on irregular repetition slotted Aloha. *IEEE Transactions on Communications*, 69(6), 3572–3585. <https://doi.org/10.1109/TCOMM.2021.3060429>
24. Chen, X., Gatsis, K., Hassani, H., & Bidokhti, S. S. (2020). Age of information in random access channels. In *IEEE international symposium on information theory (ISIT)* (pp. 1770–1775). <https://doi.org/10.1109/ISIT44484.2020.9174254>
25. Yavascan, O. T., & Uysal, E. (2021). Analysis of slotted Aloha with an age threshold. *IEEE Journal on Selected Areas in Communications*, 39(5), 1456–1470. <https://doi.org/10.1109/JSAC.2021.3065043>
26. Chen, H., Gu, Y., & Liew, S.-C. (2020). Age-of-information dependent random access for massive IoT networks. In *IEEE conference on computer communications workshops (INFOCOM WKSHPs)* (pp. 930–935). <https://doi.org/10.1109/INFOCOMWKSHPs50562.2020.9162973>
27. Kadota, I., & Modiano, E. (2021). Age of information in random access networks with stochastic arrivals. In *IEEE conference on computer communications (INFOCOM)* (pp. 1–10). <https://doi.org/10.1109/INFOCOM42981.2021.9488897>
28. Baiocchi, A., & Turcanu, I. (2021). Age of information of one-hop broadcast communications in a CSMA network. *IEEE Communications Letters*, 25(1), 294–298. <https://doi.org/10.1109/LCOMM.2020.3022090>
29. Maatouk, A., Assaad, M., & Ephremides, A. (2020). On the age of information in a CSMA environment. *IEEE/ACM Transactions on Networking*, 28(2), 818–831. <https://doi.org/10.1109/TNET.2020.2971350>
30. Neuts, M. F. (1995). *Matrix-geometric solutions in stochastic models: An algorithmic approach*. Baltimore: The Johns Hopkins University Press.
31. Akar, N., Oğuz, N. C., & Sohraby, K. (2000) A novel computational method for solving finite QBD processes. *Stochastic Models*, 16(2), 273–311. <https://doi.org/10.1080/15326340008807588>
32. Latouche, G., & Ramaswami, V. (1993). A logarithmic reduction algorithm for quasi-birth-death processes. *Journal of Applied Probability*, 30(3), 650–674.

Publisher's Note Springer Nature remains neutral with regard to jurisdictional claims in published maps and institutional affiliations.

Springer Nature or its licensor (e.g. a society or other partner) holds exclusive rights to this article under a publishing agreement with the author(s) or other rightsholder(s); author self-archiving of the accepted manuscript version of this article is solely governed by the terms of such publishing agreement and applicable law.



Kaveh Vaezi received his B.S. degree from Shahid Bahonar University of Kerman, Kerman, Iran, and the M.S. and Ph.D. degrees from Sharif University of Technology, Tehran, Iran, in electrical engineering in 2007, 2009, and 2019 respectively. Pursuing his research as a post-doctoral fellow till 2022 at the Electronics and Electrical Engineering Department, Bilkent University, Ankara, Turkey, he studied age of information (AoI) in various communication

networks. His main research interests are statistical modeling of communication networks, cooperative networks, wireless networks, learning techniques and queuing theory.



Nail Akar received his B.S. degree from Middle East Technical University, Turkey, in 1987 and M.S. and Ph.D. degrees from Bilkent University, Ankara, Turkey, in 1989 and 1994, respectively, all in electrical and electronics engineering. From 1994 to 1996, he was a visiting scholar and a visiting assistant professor in the Computer Science Telecommunications program at the University of Missouri–Kansas City, USA. He joined

the Technology Planning and Integration group at Long Distance Division, Sprint, Overland Park, Kansas, in 1996, where he held a senior member of technical staff position from 1999 to 2000. Since 2000, he has been with Bilkent University currently as a Professor of the Electrical and Electronics Engineering Department and as the Associate Dean of the Faculty of Engineering. He visited the School

of Computing, University of Missouri–Kansas City, as a Fulbright scholar in 2010 for a period of 6 months. His research interests are on performance modeling of computer and communication systems and networks, wireless networks, Internet of Things, queueing theory, and optimization.



Ezhan Karasan received the B.S. degree from Middle East Technical University, Ankara, Turkey, the M.S. degree from Bilkent University, Ankara, and the Ph.D. degree from Rutgers University, Piscataway, NJ, USA, in 1987, 1990, and 1995, respectively, all in electrical engineering. During 1995–1996, he was a Postdoctorate Researcher with Bell Labs, Holmdel, NJ. From 1996 to 1998, he was a Senior Technical Staff Member with the Light-

wave Networks Research Department, AT &T Labs Research, Red Bank, NJ. Since 1998, he has been with the Department of Electrical and Electronics Engineering, Bilkent University, where he is currently a Full Professor. From 2016 to 2022, he has been the Dean of Faculty of Engineering and the Director of the Graduate School of Engineering and Science. Dr. Karasan is currently serving as the vice-Rector of Student Affairs at Bilkent University. He has participated in FP6-IST Network of Excellence (NoE) e-Photon/ONE? and FP7-IST NoE BONE European Union projects. His current research interests are in the application of optimization and performance analysis tools for the design, engineering, and analysis of optical and wireless networks. Dr. Karasan is a member of the Editorial Board of Optical Switching and Networking journal. He was a recipient of the 2004 Young Scientist Award from Turkish Scientific and Technical Research Council (TUBITAK), a Career Grant from TUBITAK in 2004, and the 2005 Young Scientist Award from Mustafa Parlar Foundation. He received a fellowship from the NATO Science Scholarship Program for overseas studies in 1991–1994.